COMPARISON BETWEEN BIDIRECTIONAL AND HEMISPHERICAL SPECTRA OF VENUS-ANALOG BASALT-WEATHERING PRODUCT MIXTURES. C. Leight[1], M.C. McCanta[1], M. D. Dyar[2,3], J. Helbert[4], A. Maturilli[4], G. Alemanno[4], S. Adeli[4] A. Van Den Neucker[4]. [1]Dept. of Earth & Planetary Sciences, Univ. of Tennessee, 1621 Cumberland Ave., Knoxville TN 37996 (cleight@utk.edu), [2]Planetary Science Institute, 1700 East Fort Lowell, Suite 106, Tucson, AZ, 85719 [3]Dept. of Astronomy, Mt. Holyoke College, South Hadley, MA 01075, [4]Institute for Planetary Research, Deutschen Zentrums für Luft-und Raumfahrt, Berlin, Germany.

Introduction: Chemical weathering on Venus is predicted to happen solely through oxidation and sulfurization as exposed rocks interact with the CO_2- and S-rich atmosphere, with negligible hydration or physical weathering due to the lack of surface water or eolian processing. Experiments on Venus-analog basalts under CO_2 and CO_2+S atmospheric conditions have shown that common weathering products are Fe-oxides and sulfates [1,2]. The specific mineral species expected are dependent on the composition of the underlying basalt. Tholeiitic basalts weather to anhydrite ($CaSO_4$) and an Fe-oxide, likely magnetite, and high-Na alkaline basalts weather to thenardite (Na_2SO_4) and an Fe-oxide, likely magnetite [1,2]. The oxidation state of the near-surface atmosphere ($fO_2 = 10^{-20} – 10^{-21.7}$) suggests that magnetite reacts with the CO_2 atmosphere, oxidizing to hematite [3,4,5]. Chemical weathering on the surface of Venus has yet to be confirmed but has potentially been observed [6].

Bi-directional vs. hemispherical collection geometries. Common VNIR laboratory data, such as those produced at the Reflectance Experiment Laboratory (RELAB) at Brown University or included in the NASA Planetary Data System, utilize a bi-directional geometry. They employ a single incidence angle (*i*) and emergence angle (*e*), giving a static phase angle (*g*). In contrast, hemispherical geometry utilizes an integrating sphere with a single *i*, but integrates over a hemisphere of emergence angles, *e* = 0-180°.

It has long been understood that variations in *g* modulate the observed reflectance or emission from a surface [e.g., 7,8]. Previous work has also, however, found that the locations of fundamental bands do not meaningfully change for monomineralic surfaces with variations in the observational geometry and subsequent measured emissivity and reflectance [e.g. 8,9]. The effect of *g* is frequently assumed to be negligible, particularly for orbital observations [e.g., 7,10-12].

However, accurate interpretation of spectral data requires a thorough understanding of geometric effects. Orbital spectra are more like hemispherical than bi-directional data. While the sun may be treated as a point source, the assumption of a single *g* per pixel bears re-evaluation when considering km-scale pixels. Additionally, very few planetary surfaces are monomineralic. Constraining geometric effects for real geologic materials is particularly imperative for Venus, where spectral observations of the surface are limited to five atmospheric windows between 0.85 and 1.18 μm, and significant atmospheric scattering is expected [13-15].

Here we investigate two questions: (1) how does the increasing presence of optically transparent sulfates (thenardite and anhydrite) alter the spectrum of basalt in intimate mixtures? And (2) what differences between hemispherical and bidirectional spectra of these mixtures can be observed?

Methods: *Samples.* Two-phase mixtures were made from basalt and either thenardite (Na_2SO_4) or anhydrite ($CaSO_4$). Tholeiitic basalt "sand" (57% glass, 24% feldspar, 11% pyroxene, 4% Fe-Ti oxides, 3% olivine) was collected from Husavik, Iceland, and used for all mixtures for consistency. Anhydrite and thenardite were synthesized via dehydration of gypsum and mirabilite, respectively, at 100°C for >24 hrs. Anhydrite and thenardite were then ground, and both minerals and basalt were sieved to 250-500 μm. The sulfate/basalt proportion was varied to replicate weathering from a fresh basalt to a maturely altered surface. Initially, a generic basalt density and ideal end-member densities for the minerals were used to find the correct end-member masses for the volumetric proportion desired. The volumetric proportions (Table 1) have been corrected using the density of the basalt as estimated from the glass composition [16].

Table 1. Mixture labels and volume ratios.

		Volume %			Volume %
Label	Basalt	Thenardite	Label	Basalt	Anhydrite
T	0.0	100.0	A	-	100.0
BT-1	23.9	76.1	BA-1	31.6	68.4
BT-2	45.0	55.0	BA-2	53.9	46.1
BT-3	64.3	35.7	BA-3	73.5	26.5
BT-4	82.5	17.5	BA-4	88.1	11.9
BT-5	90.3	9.7	BA-5	90.3	9.7
B	100.0	-			

Spectral Collection. Bi-directional (BD) and hemispherical (HS) spectra from 0.7-2.63 μm were collected using a Bruker Vertex 80V spectrometer at the Planetary Spectroscopy Laboratory at DLR Berlin. Bidirectional data were collected with a phase angle of 30°, with a spectral resolution of 0.96 cm^{-1}. Hemispherical data utilized a gold-coated integrating sphere, with an *i = 13* °, and a spectral resolution of 0.96 cm^{-1}.

Results: BD and HS spectra of thenardite-basalt mixtures are shown in **Figure 1**. Anhydrite-basalt spectra have also been collected, and display similar trends to the thenardite-basalt mixes. Incomplete dehydration of anhydrite and thenardite can be observed in both geometries due to the presence of water bands at 1.4 and 1.9 µm.

Discussion. The samples have a wide range of reflectance values, as is expected; anhydrite and thenardite are optically transparent in the VNIR region. All of the mixtures display a non-linear increase in reflectance with increasing sulfate proportion.

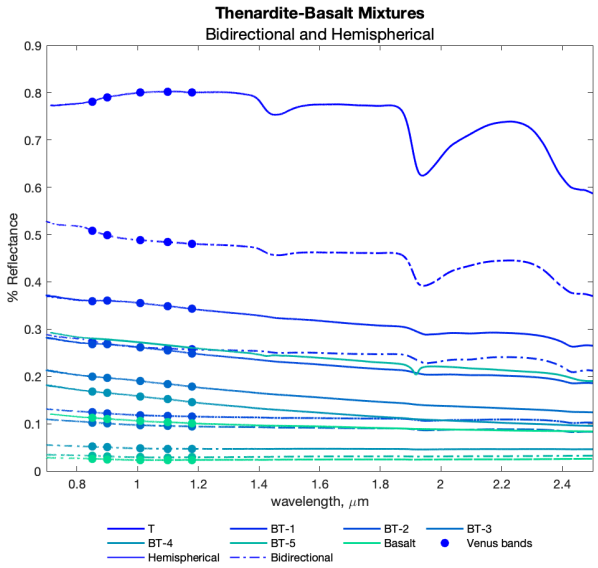

Figure 1. HS (solid lines) and BD (dashed lines) spectra of thenardite-basalt mixtures. Labels from Table 1. Solid circles show Venus atmospheric windows.

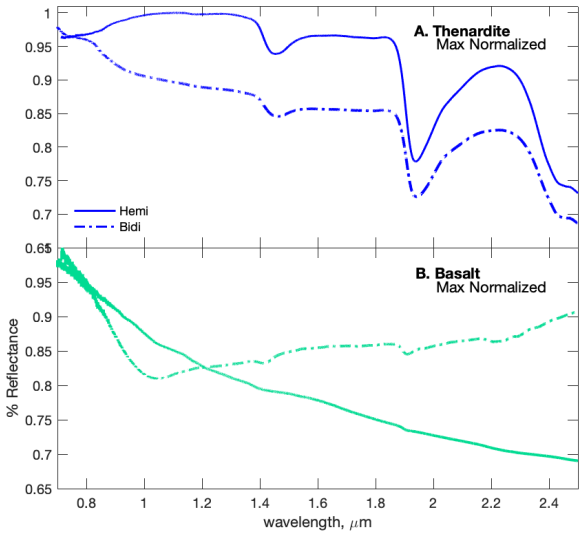

Figure 2. HS and BD spectra of thenardite and basalt with a maximum normalization.

For all samples, the HS spectrum has a higher reflectance than BD due to the different geometries. An ideal surface is an isotropic scatterer, so collecting over multiple angles allows the HS geometry to collect more reflected light than BD. While band depths are greater in HS spectra than in BD spectra, the observed band wavelengths do not change with geometry. The difference between BD and HS suggests that effects of observing geometry in laboratory measurements should not be ignored when interpreting orbital data, counter to common assumptions [e.g., 11,12].

The basalt sample has an obvious difference in spectral slope between the HS and BD spectra, with the HS spectrum displaying a near-exponential slope, decreasing with reflectance toward higher wavelengths, which virtually obscures any absorption features (Figure 2b). The sulfates and mixtures have different spectral slopes in BD and HS spectra (e.g., Figure 2a), though less dramatic than the basalt spectra, with BD spectra displaying flatter slopes, and HS spectral slope increasing in concavity with increasing basalt fraction. This difference in spectral slopes may be due to the fact that the basalt sample is not composed of a single phase, but is itself a mixture of mafic glass, plagioclase, pyroxene, oxides, and olivine, with most crystal sizes on the order of 1-100 µm.

Acknowledgments: Basalt was collected by J. Bartley, J. Tuggle, and B. Wogsland. Funded by Europlanet under the European Union's Horizon 2020 research and innovation programme under grant agreement No 871149 and by NASA grant 80NM0018D0004 to the VERITAS mission.

References: [1] Reid R. B. et al. (2021) *LPSC* LII, Abstract #2548. [2] Teffeteller H. J. et al. (2022) *Icarus,* 384, 115085 [3] Fegley B. et al., (1995), *Icarus,* 118, 2, 373-383. [4] Fegley B. et al. (1997) *Icarus,* 125, 2, 416-439. [5] Zolotov (2018) *Rev Min Geochem, 84*, 351-392. [6] Smrekar S. E., et al. (2010) *Science*, 328, 605-608. [7] Hapke, B. (1981) *JGR Solid Earth*, 86, B4, 3039-3054. [8] Wald A. E. and Salisbury J. W. (1995) *JGR Solid Earth,* 100, B12, 24665-24675. [9] Sklute E. C. et al (2015) *Am. Min.,* 100, 5-6, 1110-1122. [10] Mustard J.F. and Pieters C.M., (1989) *JGR Solid Earth,* 94, B10, 13619-13634. [11] Shkuratov Y. G. et al. (1999) *Icarus*, 137, 2, 235-246. [12] Mustard J.F. and Glotch T.D. (2020) *Remote Comp. Analysis,* 21-41. [13] Dyar M.D. et al. (2020) *GRL*, 47, 23, e2020GL090497. [14] Helbert J. et al. (2021) *Sci. Advances,* 7, eaba9428. [15] Dyar M.D. et al. (2021) *Icarus,* 358, 114139. [16] Iacovino K. and Till C.B. (2019) *Volcanica*, *2*(1), pp.1-10.